Supplementary material for

Alterations in type 2 dopamine receptors across neuropsychiatric conditions: A large-scale PET cohort

Tuulia Malén[a, b, *], Severi Santavirta[a, b], Sven De Maeyer[c], Jouni Tuisku[b], Valtteri Kaasinen[d, e], Tuomas Kankare[b], Janne Isojärvi[a, b], Juha Rinne[a, b], Jarmo Hietala[a, b, f], Pirjo Nuutila[a, b, g], & Lauri Nummenmaa[a, b, h]

[a]Turku PET Centre, University of Turku, Turku, Finland

[b]Turku University Hospital, Turku, Finland.

[c]University of Antwerp, Antwerp, Belgium.

[d]Clinical Neurosciences, Turku University Hospital and University of Turku, Turku, Finland

[e]Neurocenter, Turku University Hospital and University of Turku, Turku, Finland.

[f]Department of Psychiatry, Turku University Hospital and University of Turku, Turku, Finland.

[g]Department of Endocrinology, Turku University Hospital and University of Turku, Turku, Finland.

[h]Department of Psychology, University of Turku, Turku, Finland.

[*]Corresponding author.

Original publications whose data are used in the current study (not comprehensive)

Hietala J, Syvälahti E, Vuorio K, Någren K, Lehikoinen P, Ruotsalainen U, Räkköläinen V, Lehtinen V, Wegelius U. Striatal dopamine D2 receptor characteristics in neuroleptic-naive schizophrenic patients studied with positron emission tomography. Arch. Gen. Psychiatry 51: 116-123, 1994.

Tiihonen J, Kuoppamäki M, Någren K, Bergman J, Eronen E, Syvälahti E, Hietala J. Serotonergic modulation of D2 dopamine receptor binding in healthy volunteers in vivo, Psychopharmacology, 126: 277-280, 1996.

Hietala J, Någren K, Lehikoinen P, Ruotsalainen U, Syvälahti E. Measurement of striatal D2 dopamine receptor density and afinity with 11C-raclopride - a test-retest analysis. J Cereb Blood Flow Metab 19:219-217, 1999.

Hagelberg N, Någren K, Kajander J, Hintikka S, Hietala J, Scheinin H. μ-opiate receptor agonism increases dopamine D2 receptor binding in human basal ganglia – a positron emission tomography study. Synapse 45(1):25-30, 2002

Aalto S, Hirvonen J, Kajander J, Scheinin H, Någren K, Vilkman H, Gustafsson L, Syvälahti E, Hietala J. Ketamine does not decrease striatal dopamine D2 receptor binding in man. Psychopharmacology (Berl) 164(4):401-406, 2002.

Hirvonen J, Aalto S, Lumme V, Någren K, Kajander J, Vilkman H, Hagelberg N, Oikonen V, Hietala J. Measurement of striatal and thalamic dopamine D2 receptor binding with [11C]Raclopride, Nucl Med Comm, 24:1207-1214, 2003.

Penttilä J, Kajander J, Aalto S, Hirvonen J, Någren K, Ilonen T, Syvälahti E, Hietala J. Effects of fluoxetine on dopamine D2 receptors in the human brain: a positron emission tomography study with 11Craclopride. Int J Neuropsychopharmacol 7: 431-439, 2004.

Hirvonen J, van Erp TGM, Huttunen J, Någren K, Aalto S, Huttunen M, Lönnqvist J, Kaprio J, Hietala J, Cannon TD. Increased Caudate Dopamine D2 Receptor Availability as a Genetic Marker for Schizophrenia. Arch Gen Psychiatry, 62(4):371-8, 2005.

Hirvonen J, Karlsson H, Kajander J, Markkula J, Rasi-Hakala H, Någren K, Salminen JK, Hietala J. Striatal dopamine D2 receptors in medication-naive patients with major depressive disorder as assessed with [11C]raclopride PET. Psychopharmacology (Berl). 2008 May;197(4):581-90.

Hietala, J, Mika Hirvonen, , Jukka Huttunen, Harry Vilkman, Jussi Hirvonen, , Ville Lumme, , Kjell Någren, Pertti Neuvonen, Mikko Niemi, Raimo K.R. Salokangas. Optimization Of Antipsychotic Drug Treatment With Perphenzine –A Pharmacogenetic And Positron Emission Tomography Study. Submitted.

	N	GE Advance	HR +	HRRT	GE* VCT PET/ CT	GE* 690 PET/CT	Ecat 931
Healthy controls	239	69	13	81	9	17	50
Parkinson's disease	60	0	6	0	0	0	54
Schizophrenia	7	3	0	0	0	0	4
Violence	10	0	0	0	10	0	0
Pathological gambling	12	12	0	0	0	0	0
Depression	12	12	0	0	0	0	0
Overweight	97	38	6	16	8	27	2

Table S1. The number of subjects for each scanner in the sample. N= Number of subjects in total. GE*= GE Discovery.

Frame sequence	**N**
0 1;1 2;2 3;3 6;6 9;9 12;12 15;15 21;21 27;27 33;33 39;39 45;45 51	161
0 1;1 2;2 3;3 4;4 5;5 6;6 7;7 8;8 9;9 10;10 11;11 12;12 13;13 14;14 15;15 17;17 19;19 21;21 23;23 25;25 27;27 29;29 34;34 39;39 44;44 49	97
0 2;2 4;4 6;6 8;8 10;10 12;12 14;14 16;16 19;19 22;22 25;25 28;28 32;32 36;36 41;41 47	71
0 1;1 2;2 3;3 4;4 5;5 6;6 7;7 8;8 9;9 10;10 11;11 12;12 13;13 14;14 15;15 17;17 19;19 21;21 23;23 25;25 27;27 29;29 34;34 39;39 49	32
0 2;2 4;4 5;5 6;6 7;7 8;8 9;9 10;10 11;11 12;12 13;13 14;14 15;15 17;17 19;19 21;21 23;23 25;25 27;27 29;29 34;34 39;39 44;44 49	19
0 5;5 10;10 15;15 20;20 25;25 30;30 35;35 40;40 45;45 50	14
0 0.5;0.5 1;1 2;2 3;3 4;4 5;5 6;6 7;7 8;8 9;9 10;10 12;12 14;14 16;16 19;19 22;22 25;25 30;30 35;35 40;40 45;45 50	13
0 1;1 2;2 3;3 4;4 5;5 6;6 7;7 8;8 9;9 10;10 11;11 12;12 13;13 14;14 15;15 20;20 25;25 30;30 35;35 40;40 50	10
0 0.5;0.5 1;1 1.5;1.5 2;2 3;3 4;4 5;5 6;6 7;7 8;8 9;9 10;10 11;11 13;13 15;15 17;17 19;19 22;22 25;25 28;28 31;31 34;34 37;37 40;40 43;43 46;46 49;49 52	6
0 1;1 2;2 3;3 4;4 5;5 6;6 7;7 8;8 9;9 10;10 11;11 12;12 13;13 14;14 15;15 20;20 25;25 30;30 40;40 50	6
0 1;1 2;2 3;3 4;4 5;5 6;6 7;7 8;8 9;9 10;10 11;11 12;12 13;13 14;14 15;15 16;16 17.5;17.5 19;19 20.5;20.5 22;22 23.5;23.5 25;25 26.5;26.5 28;28 30;30 32;32 34;34 36;36 38.5;38.5 41;41 44;44 47;47 51	2
0 1;1 2;2 3;3 4;4 5;5 6;6 7;7 8;8 9;9 10;10 11;11 12;12 13;13 14;14 15;15 17;17 19;19 21;21 23;23 25;25 27;27 29;29 34;34 39;39 44	1
0 1;1 2;2 3;3 4;4 5;5 6;6 6;6 6;6 7;7 8;8 9;9 10;10 11;11 12;12 13;13 14;14 15;15 17;17 19;19 21;21 23;23 25;25 27;27 29;29 34;34 39;39 49	1
0 1;1 2;2 3;3 4;4 5;5 6;6 7;7 8;8 9;9 10;10 12;12 14;14 16;16 18;18 20;20 22;22 24;24 29;29 34;34 39;39 44;44 49	1
0 0.25;0.25 0.5;0.5 0.75;0.75 1;1 1.25;1.25 1.5;1.5 1.75;1.75 2;2 2.25;2.25 2.5;2.5 2.75;2.75 3;3 3.5;3.5 4;4 4.5;4.5 5;5 5.5;5.5 6;6 6.5;6.5 7;7 7.5;7.5 8;8 8.5;8.5 9;9 10;10 11;11 12;12 13;13 14;14 15;15 17;17 19;19 21;21 23;23 25;25 27;27 29;29 34;34 39;39 44;44 49	1
0 0.5;0.5 1;1 1.5;1.5 2;2 2.5;2.5 3;3 3.5;3.5 4;4 4.5;4.5 5;5 6;6 7;7 8;8 9;9 10;10 11;11 12;12 13;13 14;14 15;15 16;16 17;17 18;18 19;19 20;20 21;21 22;22 23;23 24;24 25;25 26;26 27;27 28;28 29;29 30;30 31;31 32;32 33;33 34;34 35;35 36;36 37;37 38;38 39;39 40;40 41;41 42;42 43;43 44;44 45;45 46;46 47;47 48;48 49;49 50;50 51;51 52	1
0 1;1 2;2 3;3 6;6 9;9 12;12 15;15 21;21 27	1

Table S2. Frame sequences of the imaging data. N= number of subjects with the frame sequence.

D_2R availability through PD duration

To assess how D_2R availability changes through PD duration, we calculated their correlation for each region in the subset of PD patients who had the disease duration information available (n= 27). Shapiro-Wilk test supported the normal distribution of the log-transformed binding potential estimates (p-value > 0.2 in each region). Thus, we used the log-transformed binding and Pearson correlation in the analysis. The test was conducted as one-tailed, because we expected negative correlation if any (binding decreases as disease progresses), due to the degenerative nature of the disease. The analyses of normality and correlation were run in RStudio (Posit team, 2023) with the R package stats (R Core Team, 2023). The correlation between PD duration and log-transformed binding was negative in all four regions: -0.44 in caudate (p= 0.01), -0.28 in accumbens (p= 0.08), -0.17 in putamen (p= 0.2), and -0.34 (p= 0.04) in

thalamus. Although age was not adjusted for in this analysis, the finding suggest that the D_2R availability decreases as PD progresses (**Figure S1**).

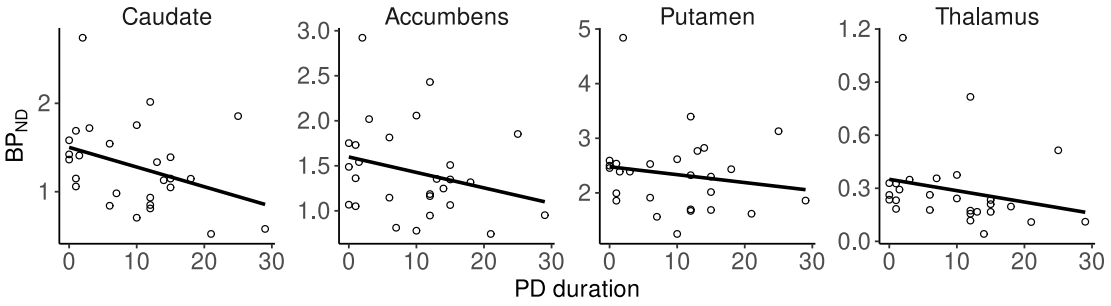

Figure S1. The BP_{ND} estimates throughout the PD duration in years (mean 10 and median 9 years, range from 0 to 29 years, for those subjects who we had the information, n=27).

	N	Mean	SD	Range	NA
Healthy controls	147	22.3	1.6	17.7-25.0	92
Parkinson's disease	11	26.8	5.1	20.3-39.4	49
Schizophrenia	2	26.9	3.0	24.1-29.7	5
Violence	10	27.2	2.3	24.0-30.7	0
Pathological gambling	12	27.8	3.4	21.2-35.9	0
Depression	12	26.5	5.2	18.9-36.5	0
Overweight	97	31.5	6.5	25.1-49.0	0

Table S3. Body mass index for the 291 subjects (67% of the total sample) for who we had the information available. N= number of observations. NA= Number of subjects with missing BMI information.

Validation of PET atlas based spatial normalization of the [^{11}C]raclopride binding estimates

Two alternative spatial normalization methods can be used to calculate binding potential (BP_{ND}) estimates from a [^{11}C]raclopride PET image: i) a deformation-field based method with Freesurfer (https://surfer.nmr.mgh.harvard.edu/) using the subject's magnetic resonance image (MRI) (Karjalainen et al., 2020), and ii) PET atlas template-based normalization with SPM (https://www.fil.ion.ucl.ac.uk/spm/) and an in-house atlas. As for the whole sample we did not have MRI available, we used the PET atlas method to maximize sample size. For validation, however, we compared the two methods. Out of the total sample (n=437), 249 subjects had MRI available. For these subjects, we assessed the similarity of their alternative BP_{ND} estimates.

To assess, how similar estimates the two normalization methods produce, we calculated the correlation between their original-scale binding estimates. We first tested the normality of the binding estimates, separately for each region within both normalization methods. As the Shapiro-Wilk test did not support normality of the binding estimates in all the tests, we used Spearman correlation. Spearman correlation was applied as one-tailed, because the variables to compare are measures of binding, and thus we expected to test only positive correlation, which was also supported in our previous work in healthy controls (Malén et al., 2022). The analyses were run in RStudio (Posit team, 2023) using the the R package stats (R Core Team, 2023).

As expected, the correlation of the alternative BP_{ND} estimates was strongest in the striatum where the reliability of [^{11}C]raclopride binding is the highest (e.g. Alakurtti et al., 2015), and despite a few outlier observations, the methods produce consistent estimates also in thalamus (**Figure S2**). The correlation was 0.88 ($p< 0.001$) in caudate, 0.89 ($p< 0.001$) in accumbens, 0.92 ($p< 0.001$) in putamen, and 0.78 ($p< 0.001$) in thalamus. The average and difference of the two methods are presented in **Figure S3**. Overall, the MRI based estimates are higher than the PET atlas based estimates, except for accumbens where the observations are more evenly represented on both sides of the zero-difference.

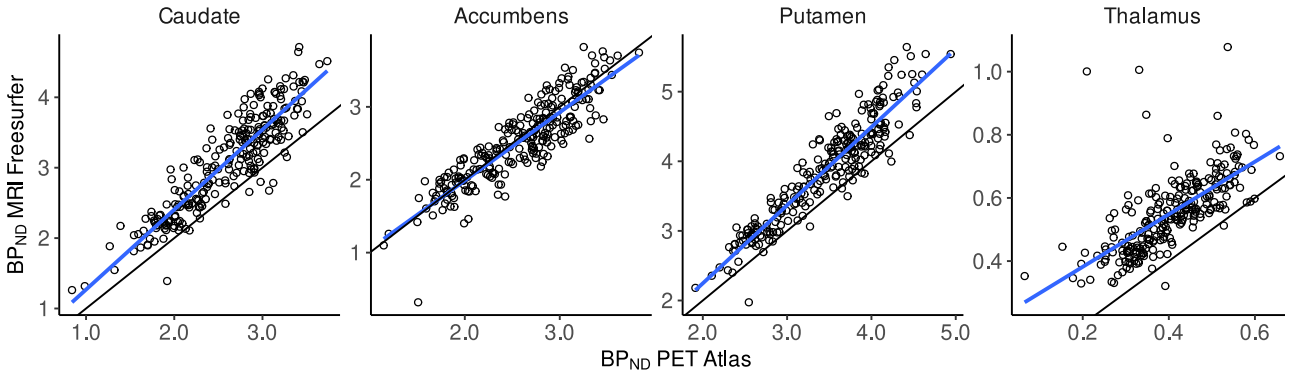

Figure S2. The association of regional [^{11}C]raclopride binding estimates from SPM with PET atlas template (x-axis), and Freesurfer with subject MRI (y-axis). The figure shows the observations of a subsample of 249 subject for who both methods could be applied. The lines represent the linear model (blue) and the y=x line (black).

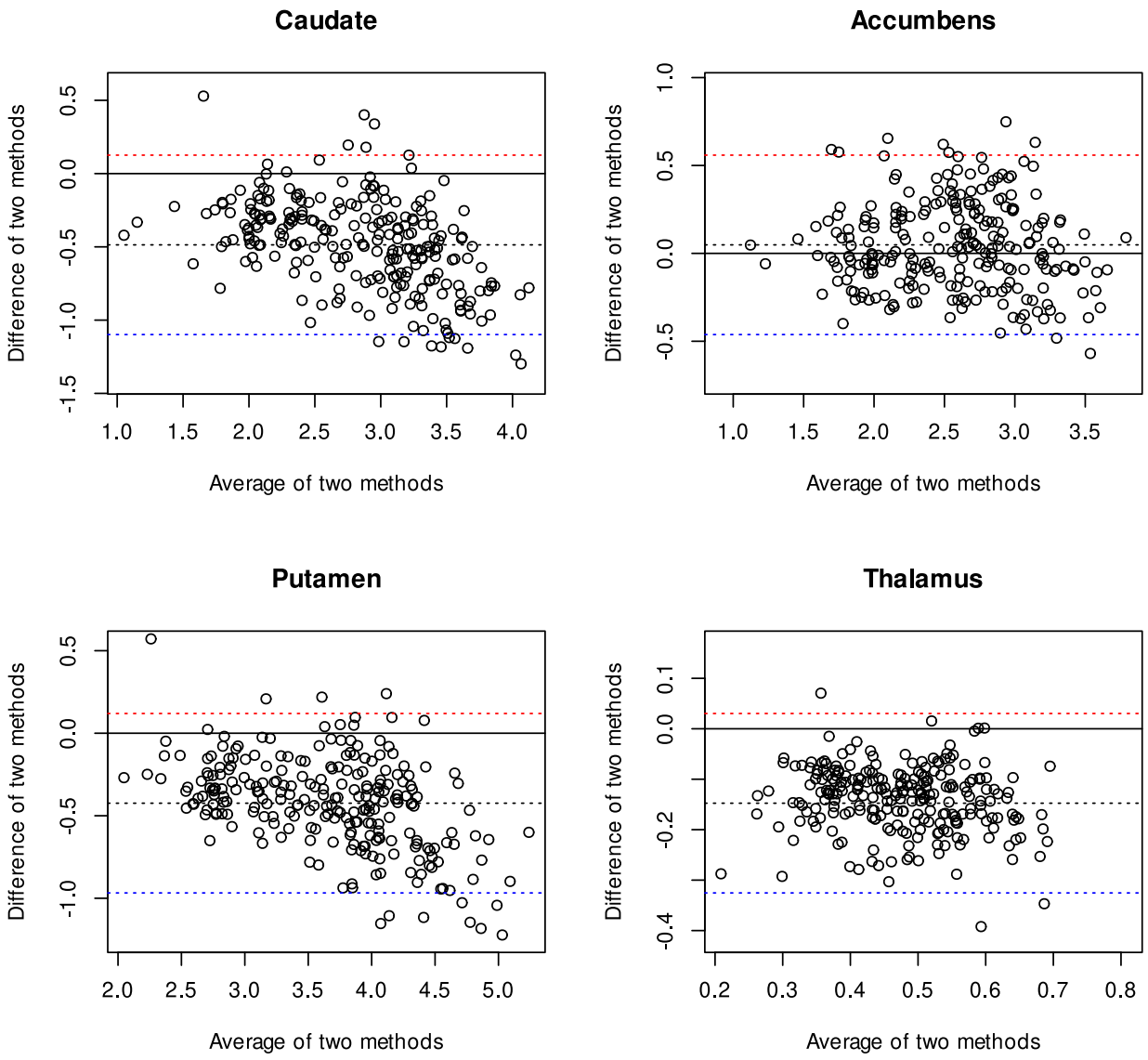

Figure S3. The association of original-scale regional [^{11}C]raclopride binding estimates from SPM with PET atlas template, and Freesurfer with subject MRI. The Bland Altman plot (Karun & Puranik, 2021) shows the average and the difference (PET atlas – MRI based estimate) of the two methods. The figure shows observations of a subsample of 249 subject for who both methods could be applied. The solid line (black) indicates zero-difference. The dashed lines represent the mean (black), the upper limit (red), and the lower limit (blue). The limits= Mean of difference + or - (1.96 × standard deviation of difference).

Left vs right

	Caudate		Accumbens		Putamen		Thalamus	
	Med. ratio	Diff range	Med. ratio	Diff range	Med. ratio	Diff range	Med. ratio	Diff range
Healthy controls	1.03	-0.40, 0.54	1.00	-0.54, 0.92	1.02	-0.21, 0.46	0.93	-0.15, 0.09
Parkinson	0.97	-0.36, 0.44	1.00	-0.83, 0.64	1.00	-0.59, 0.51	0.89	-0.15, 0.09
Schizophrenia	0.95	-0.32, 0.16	1.00	-0.39, 0.16	1.05	0.01, 0.26	0.94	-0.19, -0.00
Violence	1.01	-0.25, 0.15	0.99	-0.38, 0.39	1.01	-0.10, 0.15	0.91	-0.08, 0.01
Gambling	0.98	-0.14, 0.13	0.95	-0.29, 0.02	1.00	-0.17, 0.12	0.85	-0.12, -0.01
Depression	1.02	-0.01, 0.19	1.01	-0.14, 0.31	1.02	-0.06, 0.11	0.92	-0.12, 0.04
Overweight	1.02	-0.20, 0.27	0.98	-0.71, 0.48	1.01	-0.16, 0.59	0.93	-0.13, 0.06

Table S4. Group-specific assessment of hemispheric symmetry. Med. ratio= median of within-subject original-scale BP_{ND} ratios (left / right hemisphere). Diff range= range of the absolute within-subject original-scale BP_{ND} differences (left – right hemisphere).

Higher vs lower

	Caudate		Accumbens		Putamen		Thalamus	
	Med. ratio	Diff range	Med. ratio	Diff range	Med. ratio	Diff range	Med. ratio	Diff range
Healthy controls	1.03	0.00-0.54	1.06	0.00-0.92	1.03	0.00-0.46	1.10	0.00-0.15
Parkinson	1.08	0.00-0.44	1.10	0.01-0.83	1.04	0.00-0.59	1.16	0.00-0.15
Schizophrenia	1.06	0.01-0.32	1.07	0.00-0.39	1.05	0.01-0.26	1.07	0.00-0.19
Violence	1.03	0.01-0.25	1.03	0.00-0.39	1.01	0.00-0.15	1.11	0.01-0.08
Gambling	1.04	0.00-0.14	1.05	0.01-0.29	1.02	0.00-0.17	1.17	0.01-0.12
Depression	1.02	0.01-0.19	1.05	0.01-0.31	1.02	0.00-0.11	1.10	0.00-0.12
Overweight	1.03	0.00-0.27	1.05	0.00-0.71	1.02	0.00-0.59	1.08	0.00-0.13

Table S5. Group-specific assessment of hemispheric symmetry. Med. ratio= median of within-subject original-scale BP_{ND} ratios (higher / lower binding hemisphere). Diff range= range of the absolute within-subject original-scale BP_{ND} differences (higher – lower binding hemisphere).

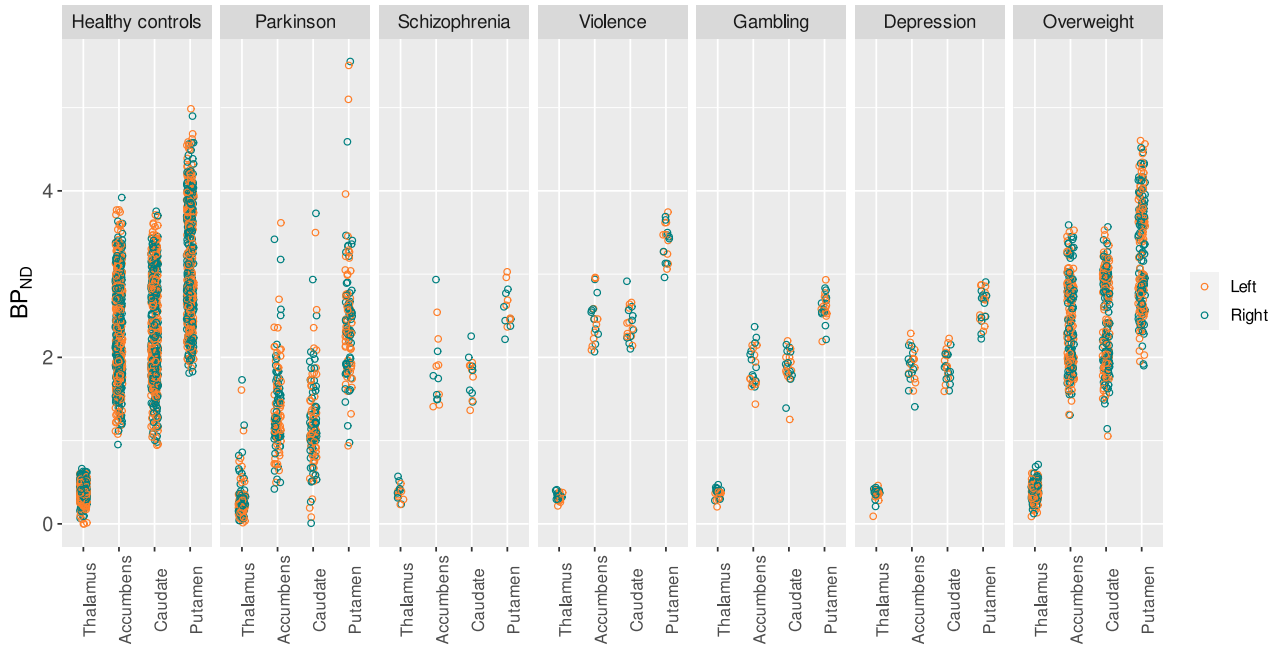

Figure S4. Left and right hemisphere original-scale BP_{ND} estimates separately for each group.

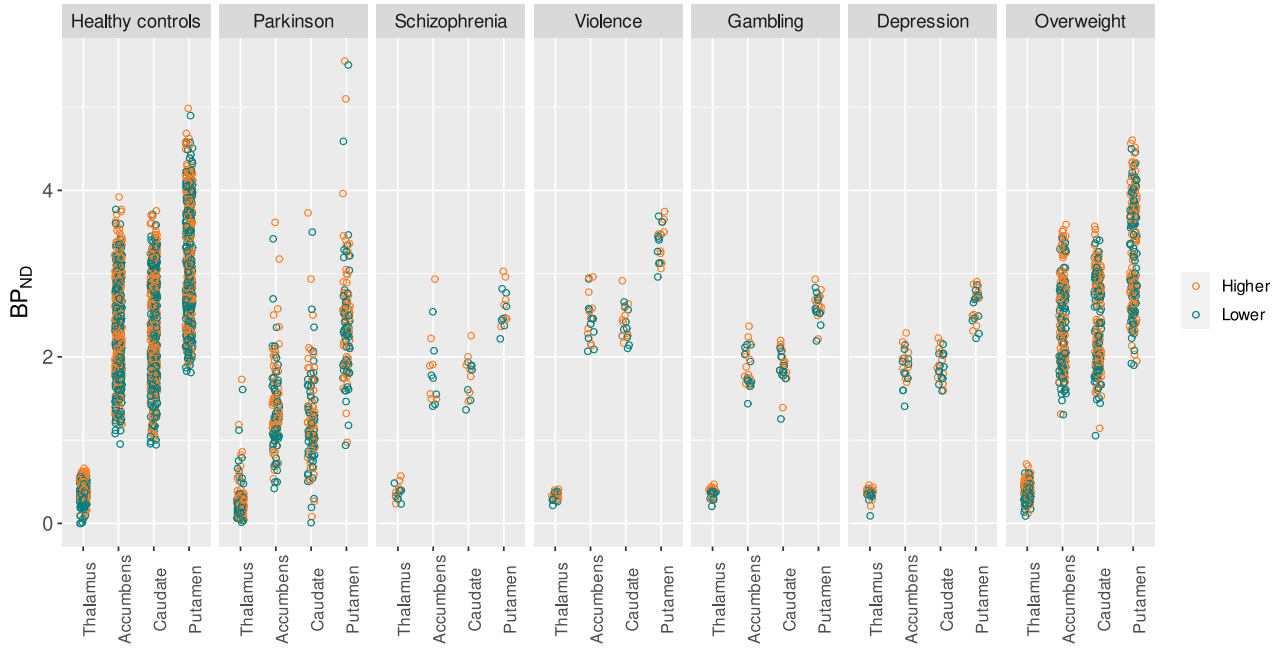

Figure S5. Higher and lower hemisphere in original-scale BP_{ND} estimates separately for each group.

Model diagnostics and comparison

In the main model, ROI was modeled as a random intercept and as a random slope for group, age, and sex effects (**Model 1**). When ROI is modeled as a random (and not fixed) effect, the model can utilize the information of the other ROIs to improve the estimates of each ROI and the non-independence of the observations across ROIs (Harrison et al., 2018). As a result, the regionally varying effects are partially pooled across ROIs (shrinkage towards the mean) (Gelman & Hill, 2006; Harrison et al., 2018; McElreath, 2020), which is also considered as a way to correct for multiple comparisons (Neath et al.,

2018). However, we only have four ROIs, while >5 levels of the random variable are recommended, and the ROIs are distinguishable units that constitute the whole population of interest (compare a random sample from a population of interest) (Harrison et al., 2018). As a result, modeling ROI as a fixed effect would also be justified (Harrison et al., 2018). Hence, we ran additional models (**Models 2-4**) with ROI as a fixed effect. More precisely, to get ROI-specific group effects, ROI was modeled as an interaction with group (instead of as a single fixed effect) in the alternative models.

Model 1 (main model):

log_bp ~ 1 + group + age_z + male + (1 | subject) + (1 | gr(scanner, id = "scanner")) + (1 + group + age_z + male | gr(roi, id = "roi")) + (1 | gr(scanner:roi, id = "scanner:roi")),

sigma ~ (1 | gr(scanner, id = "scanner")) + (1 | gr(roi, id = "roi")) + (1 | gr(scanner:roi, id = "scanner:roi"))

Model 2:

log_bp ~ 1 + age_z + male + group*roi + (1 | subject) + (1 | gr(scanner, id = "scanner")),

sigma ~ (1 | gr(scanner, id = "scanner"))

Model 3:

log_bp ~ 1 + age_z + male + group*roi + (1 | subject) + (1 | gr(scanner, id = "scanner")) + (1 | gr(scanner:roi, id = "scanner:roi")),

sigma ~ (1 | gr(scanner, id = "scanner")) + (1 | gr(scanner:roi, id = "scanner:roi"))

Model 4:

log_bp ~ 1 + age_z + male + group*roi + (1 | subject) + (1 | gr(scanner:roi, id = "scanner:roi")),

sigma ~ (1 | gr(scanner:roi, id = "scanner:roi"))

Models 1-4. Basic structure of the models using syntax of brms (Bürkner, 2017, 2018, 2021) utilizing rstan (Stan Development Team, 2020) in R (R Core Team, 2023). To help modeling convergence, maximum treedepth was set to 20 and adapt delta to the range of 0.99-0.999 (https://mc-stan.org/misc/warnings.html#divergent-transitions-after-warmup). Male indicates sex (male, female). Age_z refers to standardized age, and subject to subject index. Syntax 'gr' refers to basic grouping structure (https://rdrr.io/cran/brms/man/gr.html), applied explicitly to random variables (roi, scanner, roi:scanner) also applied to residual variances (sigma).

Main model diagnostics. Supporting sufficient convergence of the main model, there were no divergent transitions and the Rhats were 1 (Bürkner, 2017). To produce generalizable results and to avoid overfitting, we estimated how well the main model predicts new observations by running k-fold (k=3) cross-validation using brms and loo (Bürkner, 2017, 2018, 2021; Stan Development Team, 2020; Vehtari et al., 2020) packages in R (R Core Team, 2023). The cross-validation supported good specification of the main model, as the total number of parameters (here 609) was larger than the estimated effective number of parameters (p_kfold, here 534, standard error 38.3) (Bürkner, 2017, 2018, 2021; Vehtari & Gabry, 2019) indicating that the results generalize sufficiently well to unobserved data.

Model comparison. Additionally, we compared the models with the 3-fold and pareto smoothed importance sampling (PSIS) leave-one-out cross-validation (Vehtari et al., 2017) with loo package (Vehtari et al., 2020). Based on the cross-validation estimates (elpd_diff and se_diff) described by Vehtari and colleagues

(Vehtari et al., 2017), the poorest fit was Model 2, where we excluded the random effect of combined scanner and ROI (scanner:roi with 6 scanners x 4 ROIs = 24 levels). Overall, the cross-validation did not show clear signs of the alternative models being stronger at predicting new data. Thus, we reported the results of the main model specifying ROI as a random factor, coherently with our previous work (Malén et al., 2022).

Validation of the age and sex effects on regional D_2R availability

To test whether the observed effects of age (negative) and sex (higher binding in females than males) generalize outside the healthy control sample (Malén et al., 2022), we calculated these effects in two separate models predicting the BP_{ND} in i) healthy controls (n= 239, 174 males, 65 females, almost identical to the sample in our earlier work (Malén et al., 2022)), and ii) the groups of interest, including the subjects with Parkinson's disease, schizophrenia, pathological gambling, depression, past severe violent behavior, and overweight (n=198, 120 males, 78 females). For these models, we included only age and sex (and not group) as fixed effects. However, in the model analyzing the groups of interest, we allowed the intercept to vary by group (random intercept for group) to avoid the model from interpreting group-related variance in BP_{ND} as an age or sex effect. The D_2R availability decreased through age both in healthy controls about 10% in 14 years, and in the clinical groups about 10% in 17 years (**Figure S5**). On average, the decrease was about 10% in one SD ≈ 15 years (SD was 14 years in healthy controls and 17 years in the clinical groups). The age range was 19-82 in both healthy controls and in the clinical groups. Most of the probability mass supported higher binding in females than males in the healthy controls, but the difference between the sexes in the striatum was not clear in the clinical data. In thalamus, however, all subjects showed support for higher binding in females than males. Females had approximately 5% (healthy controls) and 10% (clinical subjects) higher thalamic binding than males.

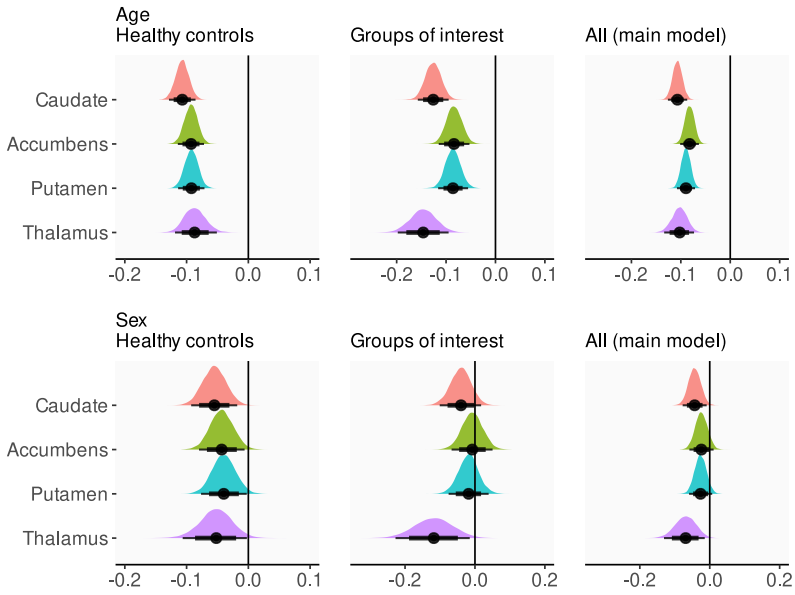

Figure S6. The effects of age (upper row) and sex (bottom row) separately among the healthy controls, the other subjects (groups of interest), and all subjects (from the main model). The x-axis shows regression coefficient of the log-transformed BP_{ND}. The effect of sex is presented as male - female, meaning negative values support higher BP_{ND} of females versus males.

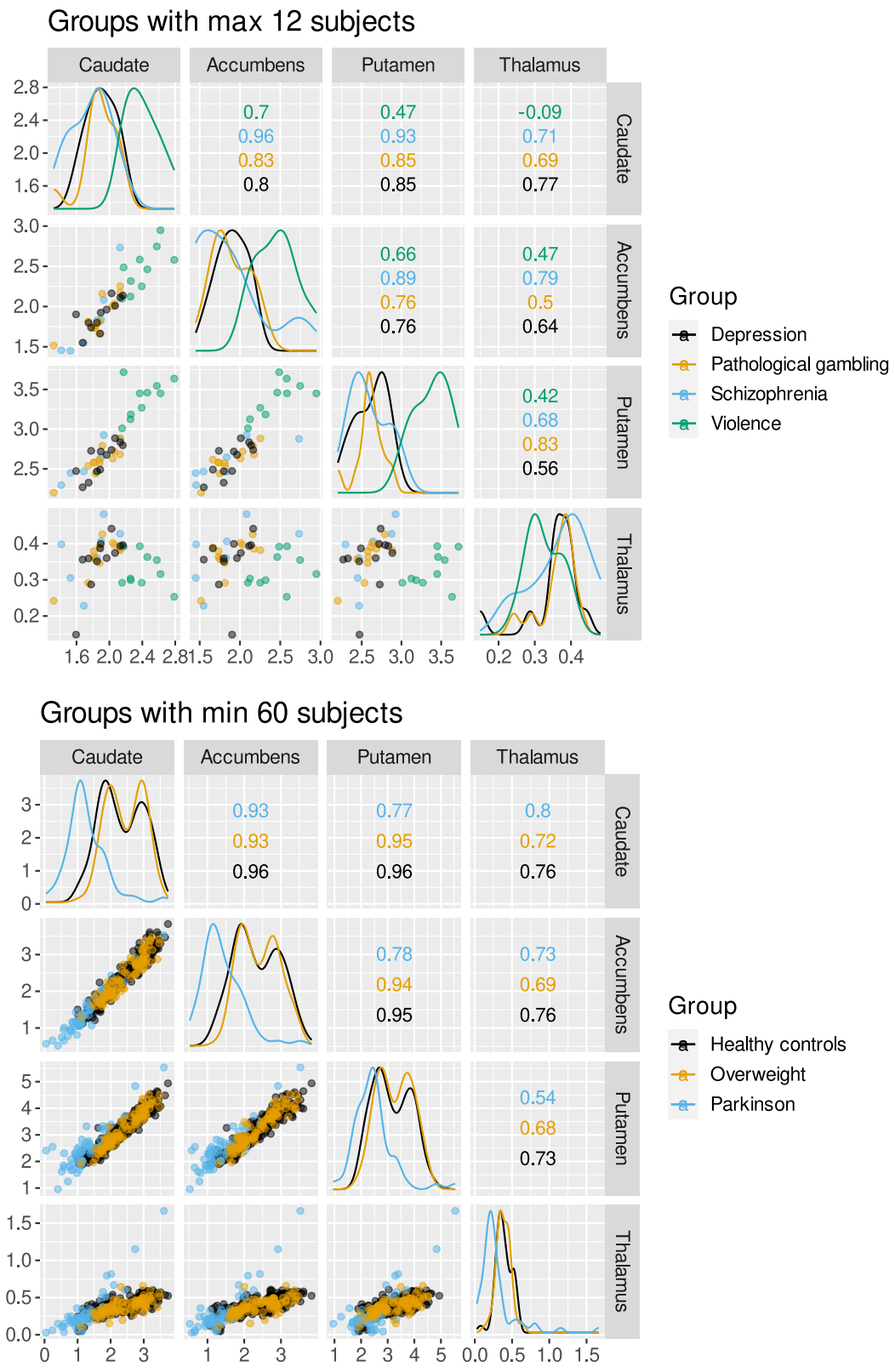

Figure S7. Between-region scatter plots (lower triangle) and correlations (upper triangle), as well as regional density plots (diagonal axis) of the original-scale BP_{ND} estimates, separately for each subject group. Small groups (maximum of 12 subjects) and larger groups (at least 60 subjects) are presented separately to enhance the visibility of the observations and their relationship between x and y axes.

References

Alakurtti, K., Johansson, J. J., Joutsa, J., Laine, M., Bäckman, L., Nyberg, L., & Rinne, J. O. (2015). Long-term test–retest reliability of striatal and extrastriatal dopamine D2/3 receptor binding: study with [11C] raclopride and high-resolution PET. *Journal of Cerebral Blood Flow & Metabolism, 35*(7), 1199-1205.

Bürkner, P.-C. (2017). brms: An R package for Bayesian multilevel models using Stan. *Journal of statistical software, 80*(1), 1-28. https://doi.org/10.18637/jss.v080.i01

Bürkner, P.-C. (2018). Advanced Bayesian Multilevel Modeling with the R Package brms. *R Journal, 10*(1). https://doi.org/10.32614/RJ-2018-017

Bürkner, P.-C. (2021, 11/30). Bayesian Item Response Modeling in R with brms and Stan. *Journal of statistical software, 100*(5), 1 - 54. https://doi.org/10.18637/jss.v100.i05

Gelman, A., & Hill, J. (2006). *Data analysis using regression and multilevel/hierarchical models*. Cambridge university press.

Harrison, X. A., Donaldson, L., Correa-Cano, M. E., Evans, J., Fisher, D. N., Goodwin, C. E., Robinson, B. S., Hodgson, D. J., & Inger, R. (2018). A brief introduction to mixed effects modelling and multi-model inference in ecology. *PeerJ, 6*, e4794.

Karjalainen, T., Tuisku, J., Santavirta, S., Kantonen, T., Bucci, M., Tuominen, L., Hirvonen, J., Hietala, J., Rinne, J. O., & Nummenmaa, L. (2020). Magia: robust automated image processing and kinetic modeling toolbox for PET neuroinformatics. *Frontiers in neuroinformatics, 14*, 3.

Karun, K. M., & Puranik, A. (2021). BA. plot: An R function for Bland-Altman analysis. *Clinical Epidemiology and Global Health, 12*, 100831.

Malén, T., Karjalainen, T., Isojärvi, J., Vehtari, A., Bürkner, P.-C., Putkinen, V., Kaasinen, V., Hietala, J., Nuutila, P., & Rinne, J. (2022). Atlas of type 2 dopamine receptors in the human brain: Age and sex dependent variability in a large PET cohort. *NeuroImage, 255*, 119149.

McElreath, R. (2020). *Statistical rethinking: A Bayesian course with examples in R and Stan*. Chapman and Hall/CRC.

Neath, A. A., Flores, J. E., & Cavanaugh, J. E. (2018). Bayesian multiple comparisons and model selection. *Wiley Interdisciplinary Reviews: Computational Statistics, 10*(2), e1420.

Posit team. (2023). *RStudio: Integrated Development Environment for R*. In Posit Software, PBC, Boston, MA. http:/www.posit.co/

R Core Team. (2023). *R: A Language and Environment for Statistical Computing*. In R Foundation for Statistical Computing, Vienna, Austria. https://www.R-project.org/

Stan Development Team. (2020). RStan: the R interface to Stan. R package version 2.21.2. http://mc-stan.org/.

Vehtari, A., & Gabry, J. (2019). Using the loo package (version>= 2.0. 0).

Vehtari, A., Gabry, J., Magnusson, M., Yao, Y., Bürkner, P., Paananen, T., & Gelman, A. (2020). *loo: Efficient leave-one-out cross-validation and WAIC for Bayesian models (Version 2.4. 1)*. In <URL: https://mc-stan.org/loo/>.

Vehtari, A., Gelman, A., & Gabry, J. (2017). Practical Bayesian model evaluation using leave-one-out cross-validation and WAIC. *Statistics and computing, 27*, 1413-1432.